Differential interference contrast microscopy for the quantitative assessment of tissue organization

Donald Duncan[*a], David Fischer[b], Mehran Dansehbod[c], Amanda Dayton[d], Scott Prahl[d]
[a]Portland State University, 1900 SW 4th Ave, Portland, OR USA 97207
[b]NASA Glenn Research Center, Cleveland, OH
[c]Dept. of Optical Science and Engineering, University of New Mexico, Albuquerque, NM USA
[d]Oregon Medical Laser Center, Providence St. Vincent Medical Center, Portland, OR USA

ABSTRACT

The propagation of light through complex structures, such as biological tissue, is a poorly understood phenomenon. Typically the tissue is modeled as an effective medium, and Monte Carlo techniques are used to solve the radiative transport equation. In such an approach the medium is characterized in terms of a limited number of physical scatter and absorption parameters, but is otherwise considered homogeneous. For exploration of propagation phenomena such as spatial coherence, however, a physical model of the tissue medium that allows multiscale structure is required. We present a particularly simple means of establishing such a multiscale tissue characterization based on measurements using a differential interference contrast (DIC) microscope. This characterization is in terms of spatially resolved maps of the (polar and azimuthal) angular ray deviations. With such data, tissues can be characterized in terms of their first and second order scatter properties. We discuss a simple means of calibrating a DIC microscope, the measurement procedure and quantitative interpretation of the ensuing data. These characterizations are in terms of the scatter phase function and the spatial power spectral density

Keywords: DIC, Nomarski, tissue characterization

1. INTRODUCTION

The propagation of light in complex, strongly-scattering random media is an important problem in diagnostic imaging and remote sensing [1-5]. Specific applications include laser communication through the atmosphere, imaging in biological media and underwater littoral regions, and imaging in extreme environments such as turbulent combustion.

Because of the complexity of the interaction in strongly scattering media (such as biological tissue), analytic physical optics methods of analysis are infeasible. In such cases, researchers have relied almost exclusively upon Monte Carlo (MC) methods based on radiative transfer theory [6-8]. Such methods employ an effective medium concept that views the medium as having certain scatter and absorption characteristics that are otherwise uniformly distributed. In other words, the medium is viewed as being homogeneous. Objects embedded within the medium (about which information may be desired) are viewed as having different scatter and absorption properties, but are otherwise assumed homogeneous as well. While this has been successful in mimicking empirical results, the method conveys no information about the actual light-matter interaction.

In a recent series of publications, we have introduced a copula-based algorithm for generating arbitrarily correlated field realizations [9]; introduced a Monte Carlo-based ray trace concept for describing propagation (including diffraction effects) in paraxial systems [10]; and a Greens function concept for propagation of coherence in high NA systems [11]. What remains is the development of structured stochastic models of the propagation medium [12]. This is the objective here. As a first step towards the development of a structured stochastic model, we discuss a means of characterizing the wavefront perturbation caused by thin tissue samples. Specifically, we discuss the use of a differential contrast interference (DIC) microscope for such a quantitative characterization

[*]duncadd1@cecs.pdx.edu; phone 1-503-725-9044; www.bme.ogi.edu/biomedicaloptics

2. MEASUREMENT CONCEPT

2.1 DIC imagery

The image produced by a DIC microscope is generally of the form [13]

$$I(x,y) = A(x,y)\left\{1-\cos\left[\phi(x+s,y)-\phi(x,y)+\Psi\right]\right\}+B(x,y) \tag{1}$$

where Ψ is a phase offset that can be adjusted by changing the bias setting on the second Wollaston prism, and by inclusion of the *A* and *B* terms we have assumed a possible amplitude effect. In this expression we have further assumed that the direction of shear is in the *x*-direction. For a small amount of shear one can write

$$I(x,y) = A(x,y)\left\{1-\cos\left[s\frac{\partial\phi(x,y)}{\partial x}+\Psi\right]\right\}+B(x,y) \tag{2}$$

If one can recover the phase gradient from the measurement, then the local ray deviation may be determined through the relationship

$$\text{ray deflection, } \theta_x = \sin^{-1}\left[\frac{1}{k}\frac{\partial\phi(x,y)}{\partial x}\right]. \tag{3}$$

For this calculation, one needs to know the amount of shear. Microscope manufacturers, however, will not provide this information. To determine this shear, we chose an object with a known phase gradient. Before discussing the details of this procedure, however, we briefly recap a particular 4-step interferometric method for recovery of phase.

2.2 Carré four-step method

The model for the Carré method is [14]

$$I_i(x,y) = a(x,y)+b(x,y)\cos\left[\phi(x,y)+\alpha_i\right]. \tag{4}$$

If one chooses the phase steps

$$\alpha_i = -3\alpha/2,\ -\alpha/2,\ \alpha/2,\ 3\alpha/2, \tag{5}$$

where α is generally unknown, but the phase steps are constant and evenly spaced, then α and the angle ϕ can be recovered from the expressions

$$\tan\left(\frac{\alpha}{2}\right) = \sqrt{\frac{3(I_2-I_3)-(I_1-I_4)}{(I_2-I_3)+(I_1-I_4)}}; \qquad \tan\phi = \tan\left(\frac{\alpha}{2}\right)\frac{(I_1-I_4)+(I_2-I_3)}{(I_2+I_3)-(I_1+I_4)}. \tag{6}$$

The beauty of the Carré method is that the phase step α may vary over the field. Once estimates of $\alpha(x,y)$ & $\phi(x,y)$ have been computed, can we recover estimates of $a(x,y)$ & $b(x,y)$? Equations 1 and 2 suggest we have four equations in two unknowns;

$$\begin{vmatrix} I_1 \\ I_2 \\ I_3 \\ I_4 \end{vmatrix} = \begin{vmatrix} 1 & C_1 \\ 1 & C_2 \\ 1 & C_3 \\ 1 & C_4 \end{vmatrix} \begin{vmatrix} a \\ b \end{vmatrix}; \qquad C_i = \cos(\phi+\alpha_i). \tag{7}$$

Multiplying both sides by the transpose of the "system" matrix, we get

$$\begin{vmatrix} \sum I_i \\ \sum C_i I_i \end{vmatrix} = \begin{vmatrix} 4 & \sum C_i \\ \sum C_i & \sum C_i^2 \end{vmatrix} \begin{vmatrix} a \\ b \end{vmatrix} \tag{8}$$

Note that (with the exception of the scalar 4) each term in Eq 7 is a full $M \times N$ matrix. Least-squares solutions of this set of equations are provided by Cramer's rule;

$$a = \frac{\det\begin{vmatrix} \sum I_i & \sum C_i \\ \sum C_i I_i & \sum C_i^2 \end{vmatrix}}{\det\begin{vmatrix} 4 & \sum C_i \\ \sum C_i & \sum C_i^2 \end{vmatrix}} \qquad b = \frac{\det\begin{vmatrix} 4 & \sum I_i \\ \sum C_i & \sum C_i I_i \end{vmatrix}}{\det\begin{vmatrix} 4 & \sum C_i \\ \sum C_i & \sum C_i^2 \end{vmatrix}} \tag{9}$$

All of the above algebraic operations are performed point-by-point.

With this measurement procedure, we thus have demonstrated the ability to recover all phase and amplitude terms in the expression describing DIC imaging. What remains is a calibration procedure that produces an estimate of the amount of shear.

2.3 Calibration concept

As discussed previously, to estimate the amount of shear produced by the microscope, we introduce an object with a known phase gradient. Towards that end, consider an optical wedge, i.e., prism that is commonly used to effect a small beam deviation (see Fig. 1).

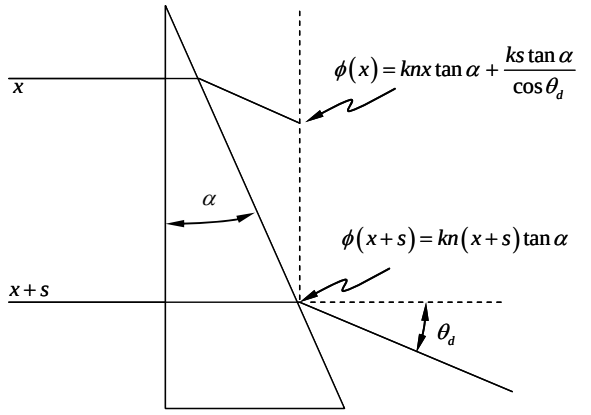

Fig. 1 Phases of rays deflected by a prism

From Fig. 1 we see that the phase difference between the two rays separated a distance s (the image shear) is given by

$$\phi(x+s) - \phi(x) = ks\tan\alpha\left(n - \frac{1}{\cos\theta_d}\right). \tag{10}$$

Now recall that the deflection angle θ_d and the wedge angle α are related through the expression

$$n\sin\alpha = \sin(\alpha + \theta_d). \tag{11}$$

We used a purported 10° wedge, i.e., a wedge that produced a 10° ray deviation. Measurement of the actual deflection at 633nm yielded an angle of 9.79°. Under the assumption that the glass was BK-7, $(n = 1.5151@\lambda = 633\text{nm})$ we arrived at a wedge angle of $\alpha = 17.8°$. For this condition, $\cos\theta_d \approx 1$ so that to a good approximation, Eq. 10 above can be written as

$$\phi(x+s) - \phi(x) = ks(n-1)\tan\alpha \tag{12}$$

Now consider Fig. 2 that illustrates the orientation of the wedge angle with respect to that of the shear. With this angle defined as θ, it's straightforward to see that the thicknesses of the wedge at the two points h_o and h_1, are related according to

$$h_1 = h_o + s\cos\theta\sin\alpha. \tag{13}$$

It follows that the complete expression for the phase difference is

$$\phi(x+s) - \phi(x) = ks(n-1)\tan\alpha\cos\theta, \tag{14}$$

where θ is the angle between the direction of the wedge and the shear.

This suggests a procedure for establishing the amount and direction of shear; acquire a series of images of a known wedge for various

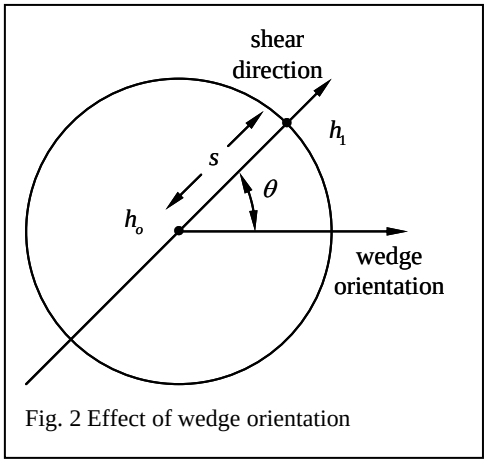

Fig. 2 Effect of wedge orientation

orientations (values of θ) and fit a model of the form shown in Eq. 1. We describe that procedure next.

2.4 Calibration procedure

We chose a series of wedge orientation angles (0°, 30°, 60°, 90°, 120°, 150°, 180°), and for each orientation captured images (at a fixed gain setting) for bias knob settings in a number of turns (0, 1, 2, 3, 4). A total of 35 measurements were made. For each orientation angle, we chose the sets of bias settings (0, 1, 2, 3) and (1, 2, 3, 4) in the Carré algorithm to calculate two estimates of the recovered phase gradient. We thus had 14 gradient estimates that were then fit to the model

$$A\left\{1+\cos\left[a\cos\left(\theta-\theta_0\right)\right]+\Psi_0-cN\right\}+B \tag{15}$$

where N is the number of turns of the bias knob on the upper Wollaston prism. Figures 3 and 4 show typical results of this procedure for a 10° wedge at 0° orientation.

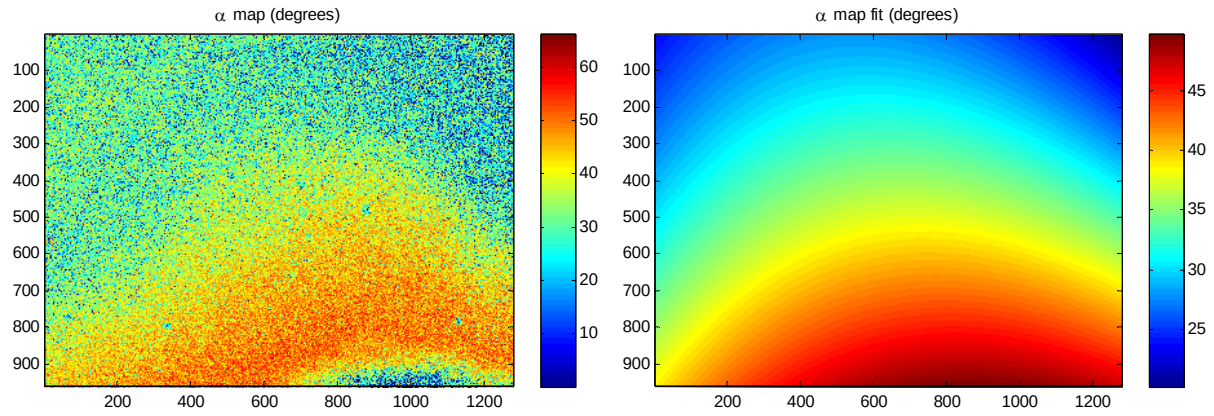

Fig. 3 Map of phase increment, α. Calculated from Eq. 6 (left); fit to valid data points (right).

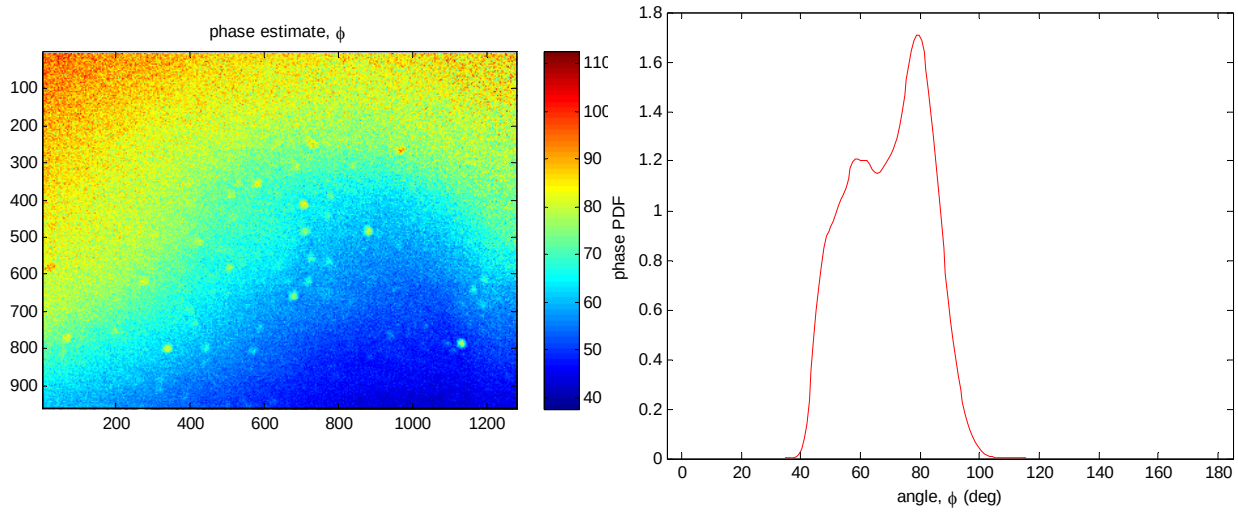

Fig. 4 Recovered phase (left) and its PDF (right).

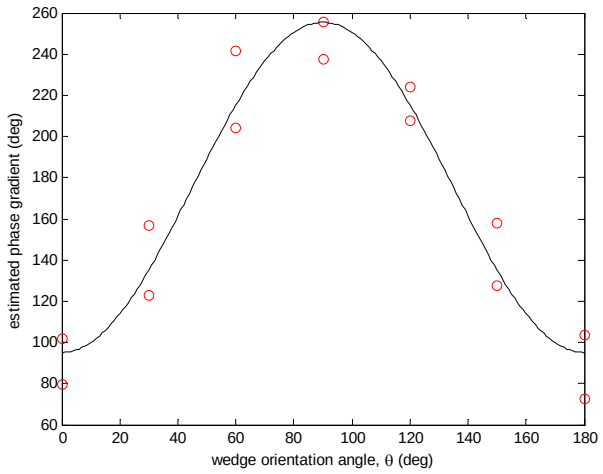

Fig. 5 Data and fit model

Note that the phase shown in Fig. 4 is actually the DIC phase difference for the wedge in this orientation. This phase distribution corresponds to an approximate $\lambda/6$ variation in flatness, which is consistent with the tolerance on the wedge. Figure 5 displays the results of fitting the data to the model shown in Eq. 15.

The fitting procedure then yields all the calibration parameters for the DIC microscope. For example, the numerical value of parameter *a* gives the shear (see Eq. 14); the parameter θ_0 yields the orientation of the shear axis; and the parameter *c* gives phase change per revolution of the bias knob.

2.5 Measurement procedure

Subsequent to the calibration procedure discussed previously, measurements on tissue sections can be performed. The phase recovered from the Carré procedure is related to the phase gradient as

$$\Phi_x(x,y) = s\frac{\partial\phi}{\partial x} \tag{16}$$

and the local ray deflection is estimated via the expression

$$\theta_x(x,y) = \sin^{-1}\left[\frac{\Phi_x(x,y)}{ks}\right] \tag{17}$$

Other azimuthal variations in the polar scatter angle are derived in a similar fashion with other sample orientations with respect to the shear axis. Alternatives, phase gradients may be extracted in two orthogonal directions,

$$\frac{\partial\phi}{\partial x} = \frac{\Phi_x(x,y)}{s} \qquad\qquad \frac{\partial\phi}{\partial y} = \frac{\Phi_y(x,y)}{s}$$

and the method of Fried [15] used to estimate the wavefront rather than the ray deflection.

3. DISCUSSION AND CONCLUSIONS

We have demonstrated a technique whereby a DIC microscope can be used to provide quantitative estimates of the local ray deflection and wavefront of a field that has propagated through a thin tissue sample. The measurement concept relies upon a prior calibration that we have described in detail. The essential feature of this calibration process is the use of an optical wedge placed at a series of known azimuthal orientations so as to provide a range of known phase gradients. Subsequent to the calibration of the microscope, we detailed a method of performing phase-stepping measurements to quantitatively assess thin tissue samples. The results that we have shown are preliminary, and there are other issues to be explored, such as the birefringence artifact. Our results, however, suggest that DIC microscopy can provide more quantitative information than is commonly assumed.

REFERENCES

[1] L. C. Andrews and R. L. Phillips, *Laser Beam Propagation through Random Media* (SPIE Press, 1998)
[2] G. Gbur and E. Wolf, "Spreading of partially coherent beams in random media," JOSA A **19**, 1592–1598 (2002).
[3] G. Yao and L. V. Wang, "Monte Carlo simulation of an optical coherence tomography signal in homogeneous turbid media," Phys. Med. Biol. **44**, 2307–20 (1999).

[4] Q. Lu, X. Gan, M. Gu, and Q. Luo, “Monte Carlo modeling of optical coherence tomography imaging through turbid media,” Appl. Opt. **43**, 1628–37 (2004).
[5] C. Mujat and A. Dogariu, “Statistics of partially coherent beams: a numerical analysis,” JOSA A **21**, 1000–1003 (2004).
[6] M. Keijzer, S. L. Jacques, S. A. Prahl, and A. J. Welch, “Light distributions in artery tissue: Monte Carlo simulations for finite-diameter laser beams,” Lasers Surg. Med. **9**, 148–154 (1989).
[7] L. Wang, S. L. Jacques, and L. Zheng, “MCML–Monte Carlo modeling of light transport in multi-layered tissues,” Computer Methods & Programs in Biomedicine **47**, 131–146 (1995).
[8] S. Bartel and A. H. Hielscher, “Monte Carlo simulations of the diffuse backscattering Mueller matrix for highly scattering media,” Appl. Opt. **39**, 1580–1588 (2000).
[9] D. D. Duncan and S. J. Kirkpatrick, “The copula: a tool for simulating dynamic speckle,” JOSA A **25**, 231–237 (2008).
[10] D. G. Fischer, S. A. Prahl, and D. D. Duncan, *Monte Carlo modeling of spatial coherence: free-space diffraction*, **J.** Opt. Soc. Am. A **25** (10), pp. 2571-2581, 2008. doi:10.1364/JOSAA.25.002571.
[11] S. A. Prahl, D. G. Fischer, and D. D. Duncan, *A Monte Carlo Green's function formalism for the propagation of partially coherent light*, J. Opt. Soc. Am. A **26** (7), pp. 1533-1543, 2009. doi:10.1364/JOSAA.26.001533.
[12] D. D. Duncan, D. G. Fischer, M. Daneshbod, and S. A. Prahl, “Differential interference contrast microscopy for the quantitative assessment of tissue organization,” Three-Dimensional and Multidimensional Microscopy: Image Acquisition and Processing XVII, SPIE Proceedings (2010).
[13] D. Murphy “Differential interference contrast (DIC) microscopy and modulation contrast microscopy,” Fundamentals of Light Microscopy and Digital Imaging, Wiley-Liss, New York, pp. 153–168 (2001).
[14] K. Creath, “Phase-measurement interferometry techniques,” in *Progress in Optics*, E. Wolf, ed. (Elsevier, Amsterdam, 1988), Vol. 26, pp. 349-393.
[15] D. L. Fried, “Least-square fitting a wave-front distortion estimate to an array of phase-difference measurements,” JOSA **67**, 370-375 (1977).